Sustainable Chemistry for Climate Action 2 (2023) 100017

Contents lists available at ScienceDirect

Sustainable Chemistry for Climate Action

journal homepage: www.elsevier.com/locate/scca

Green approach for chemical production from waste cooking oils

Jonathan Harris, Anh N. Phan*

School of Engineering, Chemical Engineering, Newcastle University, Newcastle upon Tyne NE1 7RU, United Kingdom

ARTICLE INFO

Keywords:
Waste cooking oil
Hydrocarbons
Green conversion
Gas-liquid system
Catalysis

ABSTRACT

This work demonstrates a green conversion of waste cooking oil in a continuous mode into esters, fatty acids and hydrocarbons within seconds via cold plasma catalytic approaches. Up to 60 wt.% gaseous hydrocarbons (C_1-C_6) was achieved within 11 s reaction time in hydrogen environment. Products distribution and selectivity can be easily tuned e.g. up to 43 wt.% esters (in the presence of Ni/Al_2O_3 in N_2 environment at 30 W) or up to 46 wt.% fatty acids to be obtained ($BaTiO_3$ packing under N_2 at 30 W). The selectivity of products is strongly influenced by the environment, e.g. H_2 environment promoting fatty acid methyl esters formation whereas hydrocarbons are dominant in N_2 environment.

1. Introduction

Waste cooking oil (WCO), a food waste from cooking/food processing, is commonly used to produce biodiesel (fatty acid methyl esters known as FAME) via transesterification with alcohol i.e. methanol in the presence of alkaline catalysts (e.g. KOH/NaOH). Due to the high fatty acids (FAs) content in WCOs resulting from the cooking process, pre-treatment steps are required prior to transesterification to minimize soap formation, which would cause loss of product due to difficulties in separation. In addition, the transesterification process generates around 10 wt.% waste glycerol that need to be disposed of. Thermochemical processes such as hydrotreatment and pyrolysis have been studied to convert WCOs into hydrocarbons and/or esters with or without catalysts. Catalysts for triglyceride decomposition include zeolites [1], alumina and silicates [2], sulphated zirconia and basic catalysts such as sodium carbonate. Typically, temperatures between >250–400 °C are used to maximize liquid yields [3]. The surface area and relative abundance of acid sites on the catalyst strongly affect the extent of cracking/decomposition [1]. An example is the conversion of WCO using 2.0–2.5 wt.% Co/Zn Al_2O_4 nano catalyst at 450 °C, obtaining around 67 wt.% liquid (25–25% kerosene fraction) over reaction times of 10–30mins [4].

However, these thermochemical methods, including hydrotreatment, are prone to catalyst deactivation when WCO is used as the feedstock [5], showing a noticeable drop in performance with as little as 1 h of operation [6,7]. The reaction times of thermochemical methods aimed at producing liquid fuels are also relatively long e.g. up to 6 h per batch to achieve optimum conversion [8]. Hydrotreatment of WCO is generally highly selective to hydrocarbons through favouring hydrogenation reactions (>80% oxygen atom removal from liquid) with a hydrogen co-feed of 190 ml/min H_2 for 0.33 ml/min WCO [9],which is costly and challenging to supply with current market conditions. Current studies of hydrotreatment of triglycerides have been scaled up to pilot scale and produce high yields of hydrocarbons at the cost of using large volumes of hydrogen and a long reaction time (LHSV: $2h^{-1}$).

A potential method to mitigate the long reaction time and catalyst fouling is the use of combination acid-base catalysts, which can produce 65–72% yield of liquid product within 10 min with SO_4^{2-}/TiO_2-ZrO_2 catalyst (Zhang et al., 2020). However, these combination catalysts are considered too expensive to make this a viable method at large scale. Cold plasma technologies, operating at atmospheric conditions, can rapidly convert low quality feedstock/waste into high value chemicals within a short reaction time, i.e. within seconds [10,11]. Highly energetic electrons in cold plasma (average energy of 1–10 eV from an external source), which are much higher than energy dissociation of most chemical bonds, collide with gas molecules to generate active species, which initiate reactions that could be difficult to achieve in conventional processes [12]. It was reported [13] that plasma jets were used in a batch system to produce up to 32%–70% esters from pure triglycerides over a 40–100 min reaction time. However, the process was prone to fouling when using WCO [14]. A dielectric barrier discharge (DBD) reactor can minimize the fouling issues due to its configuration and also provide flexibility in operation and ease of operation in continuous mode.

Dielectric barrier discharge reactors were used for production of biodiesel from virgin palm oil [15] and other pure triglycerides operated at temperatures of 400–500 °C [16]. These studies mainly focused on effects of operating conditions the biofuel yield/selectivity in gas-phase systems and provided limited view into the products and mechanism of the cold plasma decomposition of triglycerides. Operating at temperatures below 350 °C results in the presence of a liquid phase in

* Corresponding author.
E-mail address: anh.phan@newcastle.ac.uk (A.N. Phan).

https://doi.org/10.1016/j.scca.2023.100017
Received 22 July 2022; Received in revised form 19 January 2023; Accepted 7 February 2023

Table 1
Chemical composition of waste cooking oil and virgin rapeseed oil samples (wt.%).

Compound	WCO	Rapeseed oil
Water	0.12	0.12
Acetol	0.23	–
FA	12.43	1.27
Glycerol	1.8	–
Fatty acid esters	12.49	–
$C_{14–18}$ Hydrocarbons	1.47	–
$C_{14–18}$ Aldehydes	0.73	–
Monoglycerides	6.4	–
Diglycerides	21.24	–
Triglycerides	43.09	98.61

the reactor that can be utilized to potentially tune the process to provide high selectivity to a desired product. To address this research gap, this work focused on low temperature cold plasma conversion of triglycerides and potential catalysts for optimizing reaction rates. Cold plasma DBD was used for continuous processes with and without catalysts to directly cleave the ester bonds (to produce fatty acids) or C–C in the glycerol back bone (to generate esters and di-glycerides) or the fatty acid chains to produce hydrocarbons without pre-treatment steps in a short reaction time. Understanding the role of the carrier gas/environment, in the presence of cold plasma and catalysts on the mechanism of decomposition of triglycerides in gas and gas-liquid phase is important to optimize the process to obtain a high selectivity to the desired product(s). The findings will inform future work into a wide range of applications for this novel technique. With further work on optimizing this work, cold plasma can also be potentially scaled up either by directly increasing reactor dimensions as long as electrode separation and power supply are maintained or by using reactors in parallel to obtain faster production with a known effective reactor sizing.

2. Materials and methods

2.1. Materials

Waste cooking oil (WCO) was obtained from local restaurants at Newcastle, UK, containing only trace metals (concentration below 1 ppm) as shown in Table 1. Due to exposure to high temperatures during cooking, WCO contains a small amount of acetol (0.23 wt.%), high fatty acids (FA) (12.43 wt.%) and fatty acid esters (12.49 wt.%). WCO contains only 43.09 wt.% triglycerides (compared to 98.61 wt.% in virgin rapeseed oil) and a significant amount of di- and mono-glycerides (total: 27.64 wt.%). Fatty acid esters are known to be present in WCO at low levels due to the induction of limited pyrolysis during cooking, which produces Fatty acid esters [17].

Two environments (H_2 and N_2) in cold plasma were tested. Due to low energy excited states (3.7 eV) [18,12], hydrogen radicals are expected to be abundant and induce hydrogenation reactions. The use of H_2 as a carrier gas allows simulation of carrier gases which produce hydrogen radicals. Notably, if the gas product stream is partially recycled, the hydrocarbons present will provide hydrogen radicals, which the H_2 carrier gas data would help to understand how this would affect the process. On the other hand, N_2 can be excited to a wider range of excited states [19], thereby offering a wide range of energy levels and permitting a greater variety of reactions [20]. Inserting packing materials alters the electric field and/or surface interactions between cold plasma and catalysts which in turn influences the reaction rate and product distribution [10]. In this study, the synergetic effect of parking materials e.g. $BaTiO_3$ and common catalysts (for cracking process (e.g. HZSM-5, Faujasite HY [21,22] and zirconium oxide [23]) and for hydrogenation (Ni/Al_2O_3) and cold plasma on WCO conversion was also investigated.

2.2. Experimental method

The experimental set up was reported elsewhere [10]. A coaxial dielectric barrier discharge cold plasma reactor was used with a discharge gap of 1.5 mm and a plasma zone of length 12 cm, providing a total plasma volume of around 7.2 cm3 (Fig. 1(b)). The outer electrode was galvanised steel wire mesh whereas the inner electrode was 1 mm thick aluminium foil inside a quartz glass cover. The liquid feedstock (WCO or rapeseed oil) and carrier gas were co-currently fed into the reactor using a syringe pump (errors: ±0.01 ml/min) and a Bronkhorst mass flow controller (errors: ± 0.03 ml/min) which was mixed at a T-junction.

Prior to each experiment, the reactor was continuously purged with the selected carrier gas (H_2 or N_2) for 30 min to ensure the system was air-free (confirmed by GC analysis). As soon as the system was air-free, a known flow rate of liquid feedstock was continuously injected and mixed with the selected carrier gas at a T-mixer (Fig. 1(a)) to obtain consistent slug flow behaviour into the plasma zone. The outlet of the cold plasma reactor was connected with two condensers cooled at 0 °C to collect liquid products. The gas was analysed online every 15 min for 100 min. The liquid was collected at the end of the run for off-line analysis and for determining its yield. The gas yield was determined by relative flow rates in and out of the reactor.

The volumetric ratio of gas to liquid was varied from 20:1 to 55:1. The results showed insignificant difference from those obtained from the case of 40:1 ratio. Therefore, all experiments were fixed at a gas to liquid of 40:1 (v/v) to ensure that liquid was constantly covering the inner electrode, while preventing the reactor from flooding with liquid [10]. Each experiment was repeated at least three times to ensure reproducibility.

When the plasma zone was filled with packing materials/catalysts using a 1 mm thickness ceramic wool as the base, the reactor volume was reduced by around 37%. The packing material/ catalyst and ceramic wool disrupted the flow so that turbulence was generated, ensuring that the liquid was uniformly distributed on the material, which is desirable due to the dielectric effect [24]. As plasma discharges occur between particles, an even coverage over all surfaces prevents arcing and the associated wasted energy. Blank tests with ceramic wool only were also performed to account for these effects.

Ni/Al_2O_3 was synthesized from high surface area alumina (surface area: $180m^2/g$ particle size: 0.5 mm 99.95% purity, Alfa Aesar) and nickel nitrate hexahydrate (99.9% purity, Sigma Aldrich) via a wet impregnation method proposed by others [25,26]. The impregnated Al_2O_3 was then dried then calcined at 550 °C and hydrogenated at 550 °C, as detailed in previous work [10].

$BaTiO_3$ was purchased from Alfa Aesar at a purity of 99%, and was screened to have a particle size range of 0.5–1 mm. HZSM-5 with a SiO_2/Al_2O_3 ratio of 25:1 (Clean Energy Fuels) was pre-heat treated ($410m^2/g$ surface area, 99.95% purity). Zirconium (IV) oxide (5 μm powder, Sigma Aldrich) and Faujasite HY–zeolite (SiO_2/Al_2O_3 ratio= 3.0:1, surface area of $660m^2/g$, Alpha Aesar) were converted to the 0.5–1 mm size range by pelletizing, crushing and screening but were not pre-treated.

2.3. Analysis

Non-condensable gas outflowing directly from the quenching system was analysed online using a 3 channel Varian 450- Gas Chromatogram (GC). The GC was equipped with 2 ovens, 5 columns, 1 thermal conductivity detector for permanent gases and 2 flame ionisation detectors for hydrocarbons and alcohols. One oven housed 3 columns (Hayesep T 0.5 m x 15 m x1/8″ ultimetal, Hayesep Q 0.5 m x 1/8 “ultimetal and Molsieve 13 m X 1.5 m x1/8″ ultimetal) for permanent gas separation. The second oven housed a CP-SIL 5CB FS X.25 column for hydrocarbon analysis and a CP-WAX 52CB FS 25 m X 0.32 mm (1.2 μm) column for alcohols. The liquid yield was determined by comparing the volume of liquid input to the reactor and the volume of liquid collected at the outlet.

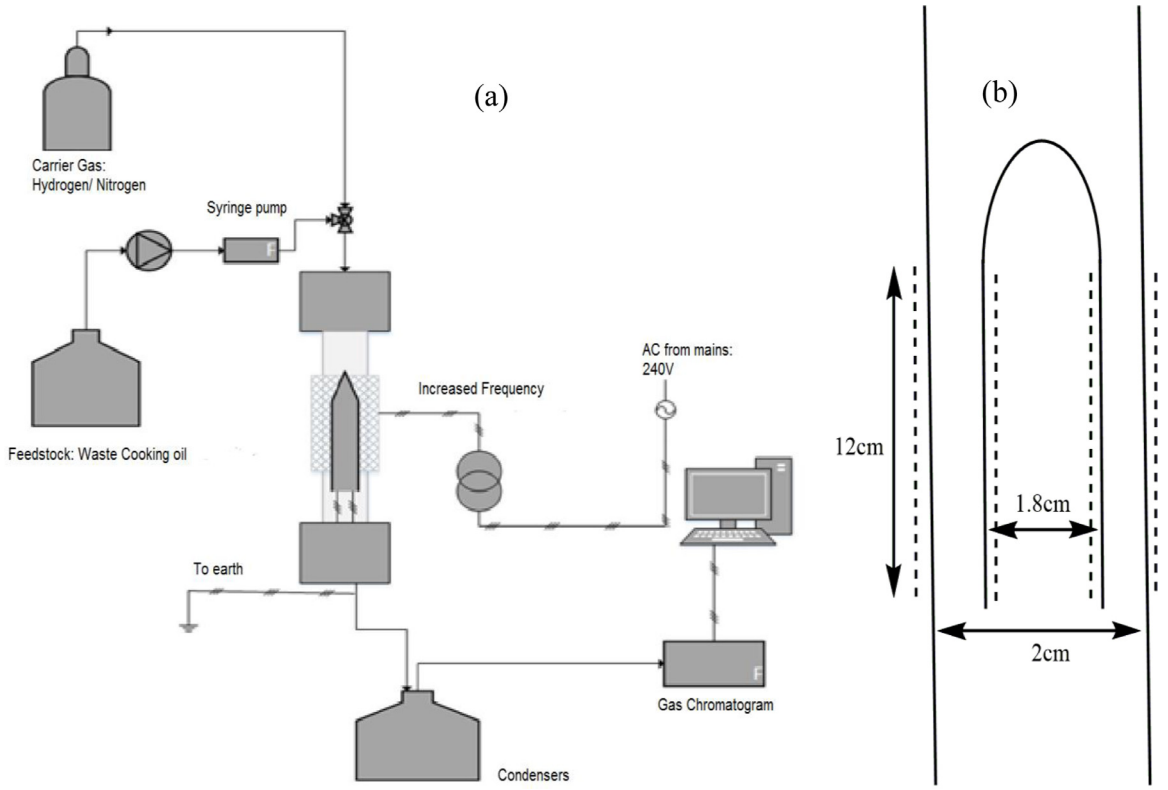

Fig. 1. (a) Experimental set-up for cold plasma induced decomposition of waste cooking oil at atmospheric pressure and temperature and (b) reactor design cross sectional diagram.

Liquid samples were fractionised into 3 separate phases containing esters and glycerides, hydrocarbons/ aldehydes and fatty acids respectively by solvent extraction. The compounds in individual fractions were identified using a Perkins-Elmer Clarus-500 with the appropriate column, then were quantified using a HP6890 GC fitted with the same column used in the GCMS. The acetonitrile soluble fraction was analysed (according to standard BS EN ISO 5508) in a HP6890 CG with a CP-Wax column to identify and quantify FAME and other fatty acid esters. The hexane fraction was also analysed in a HP6890 GC equipped with a CP-SIL 5CB FS X.25 column to determine liquid hydrocarbon/ aldehyde yields. The methanol soluble fraction was also analysed by HP6890 GC with a CP-WAX 52CB FS 25 m X 0.32 mm (1.2 μm) column to detect FA and other polar products such as acetol.

The conversion of any given run for both WCO and rapeseed oil feedstocks was defined based on the depletion of glycerides (total of mono-, di- and triglycerides) whereas yield of product was defined as a ratio of mass of product at the outlet to total mass of feedstock at inlet.

3. Results and discussion

3.1. Role of cold plasma in decomposition of triglycerides

Table 2 shows that increasing the cold plasma power increased the conversion of glycerides due to the increased concentration of excited species generated at high plasma powers [27]. The conversion was around 2 times higher in H_2 than in N_2 environment at 10 W but similar at higher plasma powers. This is because of a bell curve shape electron energy distribution and how this interacts with a gas-liquid system. As the liquid is not significantly excited by energetic electrons, initiation reactions require excitation of carrier gas molecules through collisions with energetic electrons, which limits the range of energetic states possible. Nitrogen has higher energy excited states than hydrogen, therefore at 10 W the concentration of excited species in the gas phase is limited to initiate the reaction, resulting low conversion.

The yields of fatty acids (FAs) and methane were higher in H_2 than in N_2 environment for all tested powers. This is due to the abundant hydrogen radicals in the H_2 environment promoting condensation reactions to generate FAs and the formation of methane ($CH_3\cdot + H. \rightarrow CH_4$) over propagation to form longer chain hydrocarbons ($CH_3\cdot + CH_3\cdot \rightarrow C_2H_5\cdot + H.$ or $CH_3\cdot + CH_3\cdot \rightarrow C_2H_6$). In contrast, the N_2 environment with highly energetic excited nitrogen species [20] allows more rapid cleavage of C–C/C=O bonds to hydrocarbons, H_2 and CO_2 as evidenced by higher yields of CO and CO_2 (Table 2). It can be concluded that H_2 environment is more suitable for generating gaseous hydrocarbons from triglyceride decomposition whereas N_2 environment promotes dehydrogenation reactions.

When H_2 was used as carrier gas, the yield of H_2 was the difference in hydrogen from the gas flow rates input and output and the mass fraction of hydrogen in the product gas stream. As shown in Table 2, the amount of hydrogen output exceeded the amount added as carrier gas for all tested cases. This is because hydrogen radicals can act as an initiator for glyceride decomposition reactions, which induces reactions without being depleted [28] while other plasma initiated reactions release more hydrogen radicals than were consumed, such as dehydrogenation of fatty acid chains [29].

Increasing power to 10 W to 30 W in H_2 environment, a reduction in the water yield was observed due to the decomposition of H_2O [30], which then reacts with CO/FA to form CO_2 [31,32] as evidenced by a slight increase in CO_2 (0.57 wt.% at 10 W compared to 0.84 wt.% at 30 W). The N_2 environment enhanced the dry reforming reaction between CO_2 and hydrocarbons to form H_2 and CO [33] evidenced by high CO yields (6.99 wt.% under N_2 vs 1.82 wt.% under H_2 at 50 W).

Triglycerides decompose to diglycerides, monoglycerides and glycerol along with FAs [34] via ester (C–O) (Fig. 2), which are dominant due to due to the lower bond energy of the ester bond (296 KJ/mol)

Table 2
Cold plasma assisted decomposition of triglycerides at atmospheric conditions without catalysts at a residence time of 11 s and gas to liquid ratio of 40:1 (vol/vol) at atmospheric pressure (error: ±5%).

Carrier gas	H_2			N_2		
Plasma power (W)	10	30	50	10	30	50
Conversion of triglycerides (wt.%)	33.62	39.40	51.52	17.06	33.91	50.94
Total gas yield (wt.%)	4.02	6.64	10.59	2.36	6.81	14.41
CO_2	0.57	0.84	1.69	0.71	1.02	1.90
H_2	0.83	0.99	1.47	0.92	1.46	1.89
CO	0.53	1.71	1.82	0.23	2.76	6.99
CH_4	1.80	2.67	4.84	0.39	1.11	1.85
C_2-C_6	0.29	0.43	0.77	0.12	0.46	1.80
Water	1.86	0.15	0.15	0.16	0.09	0.20
Acetol	0.90	0.12	0.45	0.02	0.03	0.09
FAs	10.97	10.25	13.61	2.83	6.25	9.48
Glycerol	0.23	0.01	0.02	–	0.01	0.01
FAME	–	0.01	0.02	–	0.01	0.02
Other esters	–	0.01	0.06	–	–	0.01
C14–18 Hydrocarbons	–	0.01	0.02	–	0.01	0.02
Monoglycerides	5.64	7.68	10.34	4.08	7.14	10.34
Diglycerides	10.00	14.52	16.26	7.61	13.54	16.16

Table 3
Cold plasma initiated WCO conversion without packing materials or catalysts at a residence time of 11 s, atmospheric conditions and a ratio of gas to liquid of 40:1 (vol/vol) (errors: ±3 wt.% for conversion, ±4% for product yields).

Carrier gas	H_2			N_2		
Plasma power (W)	10	30	50	10	30	50
Overall Glyceride Conversion (%)	2.73	7.67	30.01	−1.46	−6.04	−0.75
Total gas yield (wt.%)	4.55	5.55	17.52	3.21	4.15	4.01
CO_2	–	–	–	1.58	1.93	2.13
H_2	–	–	–	0.06	0.05	0.04
CO	–	–	–	0.99	1.59	1.28
CH_4	4.55	5.55	13.16	0.44	0.39	0.48
C_2-C_6	–	–	4.35	0.15	0.19	0.30
Liquid (wt.%)						
Water	4.25	1.83	0.36	2.70	1.63	1.97
Acetol	0.28	1.47	12.42	0.89	0.39	0.03
FAs	12.47	7.23	4.54	5.15	5.80	10.18
Glycerol	1.78	1.99	–	–	–	0.98
FAME	2.31	4.21	4.49	3.42	4.24	2.21
Other esters	4.12	6.23	5.35	9.47	6.29	4.82
$C_{14–18}$ Hydrocarbons	0.93	0.98	0.84	1.69	1.23	1.88
$C_{14–18}$ Aldehydes/ketones	0.89	0.95	0.83	1.71	1.27	2.46
Monoglycerides	11.13	11.12	9.71	7.66	4.22	1.25
Diglycerides	11.68	23.13	15.79	25.93	33.76	24.74
Triglycerides	45.61	35.30	28.16	38.17	37.02	45.27

[35], and C–C bond splitting (Fig. 2). Splitting of the fatty acid chains to produce short chain hydrocarbons also occurred but did not dominate under any carrier gas/ plasma power combination.

3.2. Conversion of WCO in the presence of cold plasma

In the N_2 environment at atmospheric temperature, the glyceride conversion was negative (Table 3). A plausible explanation is due to the lower rate of de-esterification (decomposition) than that of esterification [36]. This is evidenced by a sharp decrease in FA content (from 12.43 wt.% in the feedstock (Table 1) to 5.80 wt.% at 30 W) and no glycerol detected at 10–30 W (Table 3). At 50 W, an increase in glycerol and FA yields suggests that the decomposition of glycerides dominated over the esterification reaction. Referring decomposition of virgin rapeseed oil in a N_2 environment (Section 3.1), the conversion of triglycerides increased with increasing cold plasma power.

In the H_2 environment, the conversion of glycerides was around 30% at 50 W to produce up to 17.52 wt% gaseous hydrocarbons. The absence of CO and CO_2 indicates that the abundant hydrogen radicals prevent cracking and dehydrogenation of carboxylic or alcohol groups. A similar result was observed during hydrogenation of WCO at 120 °C with supercritical propane (183 bar) [37]. At 10 W in the H_2 environment (Table 3), although the total glyceride content in the output remained similar to the feedstock, products were formed e.g. FAME (2.31 wt.%), other fatty acid esters (4.12 wt.%), FA (12.47 wt.%), methane (4.55 wt.%) and water (4.25 wt.%). This can be explained due to cracking reactions throughout the glyceride molecule. Gas yield increased significantly (from 5.55 wt.% to 17.52 wt.%) when plasma power increased to 30 to 50 W. An increase in acetol yield at 50 W plasma power (12.42 wt.% from 1.47 wt.% at 30 W) indicates extensive de-esterification of glycerides to generate glycerol which then decomposes to acetol [10]. This is supported by a decrease in the total glyceride content (mono-, di- and triglycerides) from 68.42 wt.% at 10 W to 53.66 wt.% at 50 W (Table 3). Methane was the only hydrocarbon generated at 10–30 W under H_2, due to the hydrogen radical concentration promoting the termination reactions (CH_3 + H= CH_4). The high yields of fatty acid esters and FA with the reduced total glyceride contents in H_2 (Table 3) compared to the feedstock suggests that H_2 is effective for decomposition of glycerides. In contrast, N_2 preferentially deoxygenates as evidenced by the formation of carbon oxides.

In conventional thermal decomposition, the conversion was below 20% at a tested temperature range of 250–300 °C (Table 4). Increasing temperatures from 250 °C to 300 °C slightly increased the conversion of glycerides for both cases of carrier gas (H_2 and

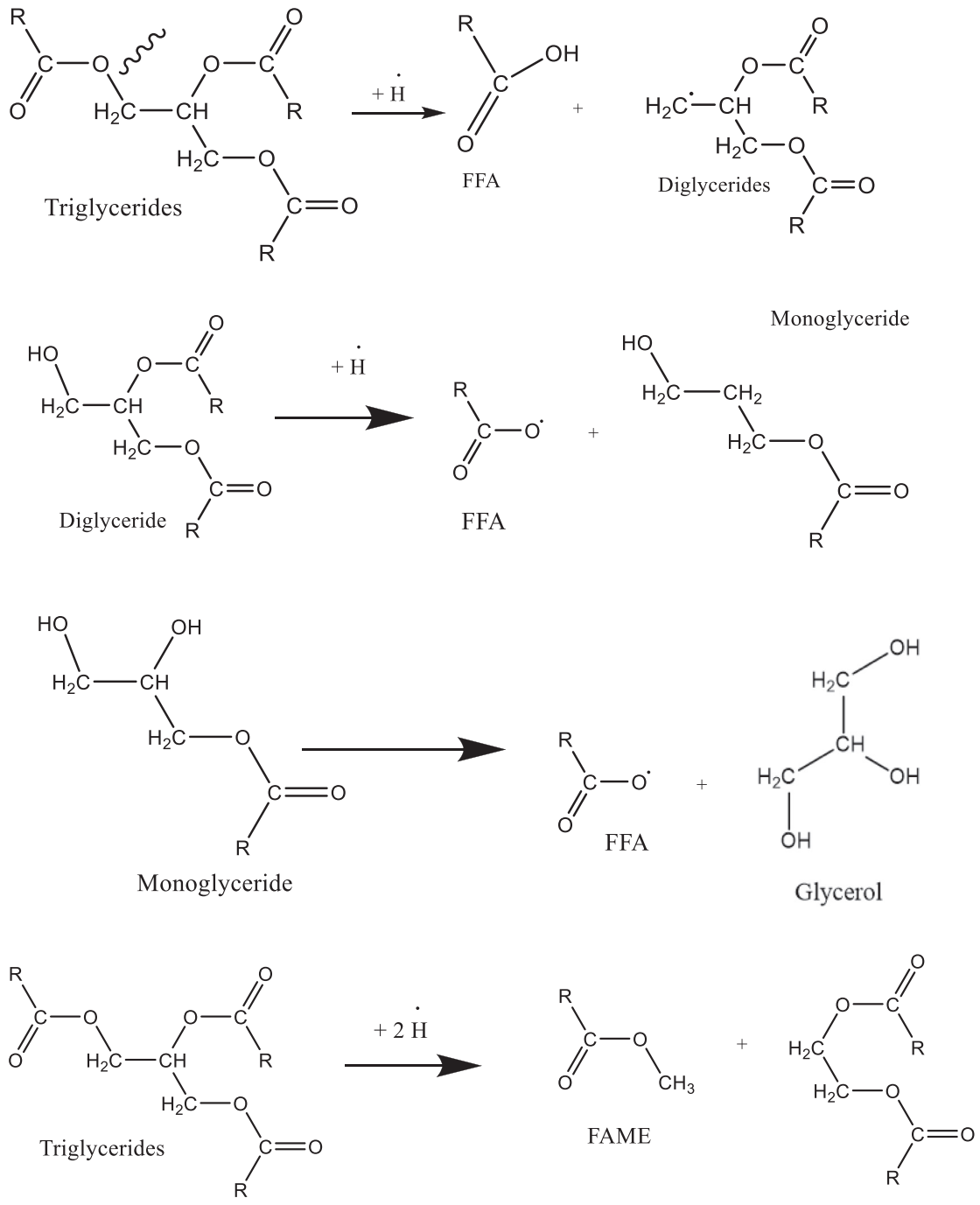

Fig. 2. De-esterification of glycerides. Cracking glycerides to generate FAME.

N_2). The high yield of water observed for thermal decomposition (Table 4) provides strong evidence of glyceride dehydration to FA and glycerol.

In the presence of cold plasma at 50 W, increasing the temperatures significantly increased the conversion of glycerides and gaseous hydrocarbons (Tables 3 and 4). This is because the reaction now is in the gas phase rather than at the interface gas-liquid. In the H_2 environment, high yields of esters, FAs and gaseous hydrocarbons (up to 58.8 wt.% at 300 °C) but negligible acetol were observed compared to results from the N_2 environment. This is expected as acetol formation can be prevented by hydrogen radicals [38]. The N_2 environment also produced a high yield of hydrocarbons (around 40 wt.%) in the gas phase with predominantly FAs in the liquid phase.

3.3. Effects of packing material and catalysts in the presence of cold plasma

Table 5 shows that packing $BaTiO_3$ in the cold plasma under H_2 promotes the decomposition of triglycerides. The glyceride conversion in the presence of Ni/ Al_2O_3 was much lower than that in $BaTiO_3$ (31.05% vs 52.88% at 30 W in N_2 environment). This is because Ni/ Al_2O_3 favours C–C bond cracking reactions [25], which reduces fatty acid chain lengths, generating FAME (e.g. 31.3 wt.% at 30 W in N_2) whereas $BaTiO_3$ induces de-esterification to form FAs (57.85 wt.% under $BaTiO_3$ vs 3.73 wt.% Ni/ Al_2O_3 at 30 W). Thermal assisted hydrodeoxygenation of glycerides requires 380–420 °C, 10–20 bar H_2 and a catalyst (i.e. sulphated zirconia or HZSM-5) over hours to produce e.g. FAME alongside carbon oxides [23]. Increasing residence time from 7 s to 11 s increased

Table 4
Comparison of thermal decomposition and combined heating/cold plasma of WCO at 11 second residence time and a 40:1 gas to liquid ratio (errors: 5%).

	Thermal only				Thermal + 50 W plasma			
Carrier gas	H_2		N_2		H_2		N_2	
Temperature (°C)	250	300	250	300	250	300	250	300
Glyceride Conversion (%)	2.08	12.11	2.63	16.20	54.72	63.99	26.66	81.45
Total gas yield (wt.%)	1.40	1.34	5.63	3.45	28.95	69.23	23.88	50.33
CO_2	–	0.42	–	1.70	1.32	4.50	2.96	3.92
H_2	–	0.01	–	–	–	–	2.58	1.18
CO	–	0.32	–	0.31	2.44	5.84	8.82	5.85
CH_4	0.84	0.08	3.38	0.36	7.68	10.52	3.93	5.60
C_2	0.56	0.06	2.25	0.59	4.89	18.34	1.73	13.28
C_3	–	0.26	–	0.38	9.32	21.71	3.26	14.96
C_4	–	0.13	–	0.10	2.05	5.28	0.46	3.46
C_5	–	0.03	–	0.01	1.13	2.74	0.12	1.95
C_6	–	0.03	–	–	0.10	0.21	0.03	0.12
Liquid (wt.%)								
Water	15.74	22.43	13.75	25.82	0.07	0.04	0.09	0.04
Acetol	0.54	1.36	0.77	1.88	0.46	0.17	5.72	1.94
FAs	10.81	8.58	10.38	9.42	9.57	9.74	24.60	12.33
Glycerol	1.86	4.04	0.47	0.13	0.33	0.01	0.19	0.03
FAME	0.09	0.02	0.03	–	7.15	9.63	3.68	0.47
Other esters	0.25	0.05	0.10	0.02	10.17	6.95	1.80	0.28
C14–18 Hydrocarbons	0.02	0.01	0.01	–	0.50	0.96	0.51	0.10
C14–18 aldehydes/ketones	0.04	0.01	0.01	–	0.51	0.97	0.47	0.06
Monoglycerides	10.12	8.10	12.35	9.22	18.83	19.20	28.84	9.15
Diglycerides	11.64	17.42	19.88	19.72	10.40	4.79	14.85	3.03
Triglycerides	47.50	36.64	36.64	30.33	2.80	1.48	8.18	0.91

Table 5
Cold plasma initiated WCO decomposition at atmospheric temperature with packing material/catalyst at a residence time of 7 s and a 40:1 liquid to gas ratio (vol/vol) (errors±5%).

Catalyst/packing materials	$BaTiO_3$			$BaTiO_3$			$BaTiO_3$	Ni/Al_2O_3			Ni/Al_2O_3		
Carrier gas	H_2			N_2			N_2 *	H_2			N_2		
Plasma power (W)	10	30	50	10	30	50	50	10	30	50	10	30	50
Glyceride conversion (%)	0.34	14.68	33.17	2.53	52.88	43.77	77.9	−1.36	−0.66	1.41	2.35	31.05	12.33
Total gas yield (wt.%)	11.82	13.78	16.69	3.01	4.91	6.28	10.96	1.83	3.41	4.59	4.41	5.99	9.15
CO_2	–	–	–	1.96	4.09	4.70	7.58	1.75	1.64	2.20	1.24	4.24	4.40
H_2	0.02	0.26	0.26	0.12	0.19	0.95	1.24	0.02	0.05	0.06	0.80	0.21	0.23
CO	–	–	–	0.60	0.34	0.18	0.58	0.07	0.99	1.33	1.17	0.74	2.68
CH_4	11.81	12.15	14.32	0.32	0.26	0.41	1.23	–	0.44	0.59	0.90	0.53	1.40
C_2	–	1.07	1.62	0.02	0.03	0.03	0.29	–	0.22	0.29	0.22	0.17	0.28
$C_{3–5}$	–	0.29	0.50	–	0.01	0.01	0.04	–	0.08	0.13	0.08	0.10	0.17
Liquid yield (wt.%)													
Water	0.15	0.15	0.10	0.24	0.15	0.13	1.48	2.19	1.17	0.13	0.16	0.13	0.14
Acetol	0.90	0.05	0.08	–	–	0.14	0.41	0.61	–	–	0.91	0.42	0.76
FAs	7.67	6.40	13.93	17.86	56.85	45.65	53.89	15.81	10.26	7.44	10.41	3.73	2.95
Glycerol	0.05	0.16	0.18	0.12	1.12	0.24	0.83	0.16	0.83	0.03	0.71	0.05	–
FAME	2.41	6.69	6.31	2.75	1.44	0.93	1.34	2.19	4.45	6.08	6.95	31.30	22.72
Other esters	4.77	10.58	13.51	5.46	5.30	5.79	7.72	5.42	7.57	9.98	6.83	9.05	2.19
$C_{14–18}$ Hydrocarbons	0.88	0.93	0.97	0.80	0.63	0.53	6.92	0.05	0.67	0.78	0.31	0.29	0.03
$C_{14–18}$ Aldehydes	0.86	0.91	0.96	0.82	0.64	0.51	0.82	0.05	0.44	0.53	0.24	0.28	0.02
Monoglycerides	27.40	14.92	19.97	45.18	14.55	11.23	6.22	1.99	9.40	27.34	9.32	25.99	36.40
Diglycerides	24.90	31.25	15.23	13.99	13.39	21.34	6.82	35.87	35.13	28.19	25.26	17.31	21.10
Triglycerides	18.19	14.18	12.07	9.77	5.39	7.20	2.59	33.83	26.67	14.91	36.57	5.47	4.51

* 11 second residence time.

the conversion from 43.77% to 77.91% at 50 W in N_2 for $BaTiO_3$. This is due to more extensive cracking reactions at the longer residence time [39].

Fig. 3 shows that in H_2 environment, FA chain length was almost the same as that in the feedstock. In contrast, the chain length decreased significantly in the N_2 environment e.g. no trace of C20 without packing, while C18 and C20 chain lengths disappeared in the case of 50 W with the Ni/ Al_2O_3 catalyst due to catalytic cracking. $BaTiO_3$ has little effect on chain length compared to the no packing runs.

Table 6 below shows the results of zirconia, HZSM-5 and Faujasite Y (Y-Zeolite) catalysts on cold plasma initiated WCO decomposition. Without external heating, the gas yield was low for all catalysts (i.e. less than 25 wt.%) and the chemical composition of the liquid phase was relatively unaffected, with reduced FA/FAME yields as the only major change (15.74 wt.% in the feedstock to 11.14 wt.% for zirconia). The pore size of the zeolite catalysts play an important role. Zeolites are known to induce cracking reactions at acidic active sites inside the material, with less than 1% of the acid sites visible on the external surface [11]. However, the pore size of the zeolites in this study (HZSM-5 has pores of 0.55–0.56 nm and Faujasite HY (Y-Zeolite) has 0.76 nm pores) [40,41]) were much lower those of fatty acids (a length of >1.97 nm) and triglyceride (three fatty acids bonded in parallel to a 0.29 nm diameter glycerol molecule (2018)). Triglyceride molecules thus would not fit into the pores, limiting catalysed cracking reactions to external acid sites. The results in Table 6 indicate that zirconia and zeolites promote the decarbonylation/decarboxylation of WCO as evidenced by the high

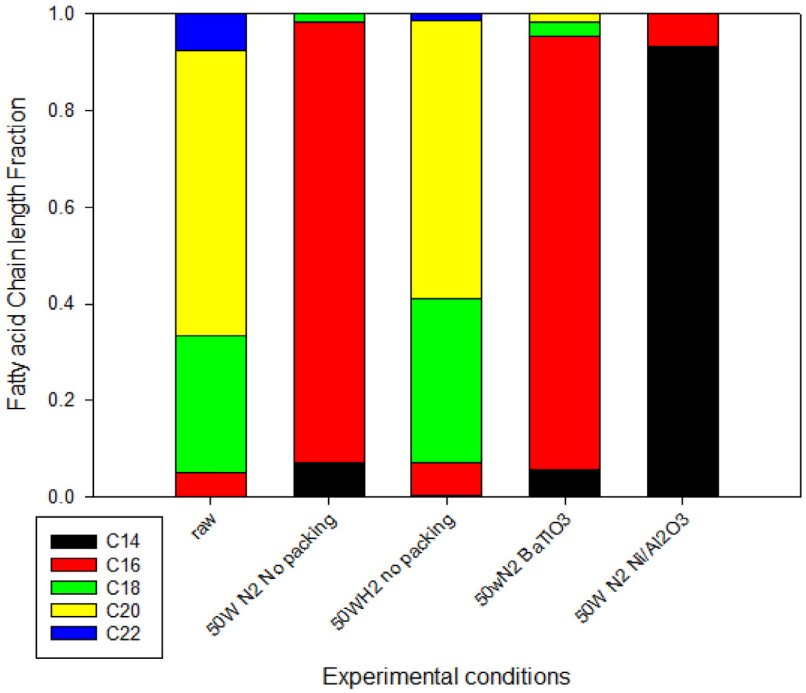

Fig. 3. Fatty acid chain length distribution for waste cooking oil and cold plasma decomposition products for various operating conditions.

Table 6
Cold plasma initiated WCO decomposition in N_2 environment at a residence time of 7 s with selected catalysts and 50 W plasma power at a gas: liquid ratio of 40:1(vol/vol) (errors: ±5%).

Catalyst	Zirconia		Y-Zeolite		HZSM-5
External heating (°C)	N/A	300	N/A	300	N/A
Glyceride conversion (%)	18.78	72.51	11.93	68.36	28.74
Total gas yield (wt.%)	11.11	43.56	2.13	49.94	23.37
CO_2	2.67	12.80	–	9.48	4.49
H_2	1.58	0.19	0.93	0.50	2.51
CO	5.32	13.50	–	8.96	10.30
CH_4	1.26	7.39	1.05	2.43	4.49
CH_2O	–	0.12	–	3.49	–
C_2	0.13	7.87	0.08	9.39	1.50
C_3	0.13	1.53	0.07	5.62	0.08
C_4-C_7	0.01	0.56	0.01	3.50	0.01
Liquid (wt.%)					
C_7-C_9	–	–	–	0.1	–
Water	0.22	0.05	0.25	0.87	0.33
Ethanal	–	0.43	–	1.27	–
Propenal	–	1.55	–	2.67	–
Acetol	0.08	0.12	–	0.05	0.06
FAs	4.06	2.13	7.80	5.48	1.30
Glycerol	0.53	0.03	1.55	0.54	0.01
FAME	7.08	12.41	5.56	4.72	10.19
Other fatty acid esters	8.44	15.30	8.80	7.00	3.89
C14–18 hydrocarbons	0.94	1.16	0.67	1.15	1.59
Monoglycerides	8.86	13.24	6.64	11.97	9.64
Diglycerides	20.01	6.52	22.25	8.03	18.04
Triglycerides	38.67	3.10	44.35	6.31	31.58

yields of CO_2 and CO. Hydrogen yields are also elevated when operated at ambient temperature, while the decrease in hydrogen yields at 300 °C is likely due to hydrogenation reactions.

When external heating was applied, the performance of the catalysts was comparable to that of $BaTiO_3$ under the same conditions (300 °C with 50 W in N_2 environment). Zirconia produced high yields of FAME (12.41 wt.%) and esters (15.30 wt.%) compared to zeolites. CO_2 (12.80 wt.%) and CO (13.50 wt.%) yields were also increased with the external heating. Hydrocarbons generated at 50 W was greatly increased by heating (17.35 wt.%). Ni/Al_2O_3 produced higher yields of hydrocarbons (56.11 wt.% vs 17.35 wt.%) but the average chain length was longer than that for zirconia (2.6 for Ni/Al_2O_3 vs 1.7 for zirconia), which implies zirconia is more effective at inducing cracking reactions than Ni/ Al_2O_3 under N_2 environment cold plasma.

The residual glyceride (mono, di and triglycerides) (67.54 wt.%) and FA (4.06 wt.%) (50 W N_2, Table 6) contents after plasma treatment without heating were higher for zirconia than for Ni/Al_2O_3 catalysed experiments (5.91 wt.% and 3.38 wt.% respectively). This indicates that the catalytic activity of zirconia is lower than Ni/ Al_2O_3. However, unlike Ni/ Al_2O_3, zirconia does not lose catalytic activity within the observed experimental time. This means that if the catalytic activity of zirconia could be improved, it may be useful for modifying process se-

lectivities without catalyst deactivation or requiring a longer residence time.

Referring to conventional catalytic decomposition where the highest WCO conversion observed (68%) with a 59 wt.% yield of FAME was achieved with sulphated zirconia at 300 ˚C over 2 h, cold plasma with a zirconia catalyst and external heating to 300 ˚C converted 72.51% around 7 s (Table 6) to produce 12.41 wt.% FAME, 15.30 wt.% other esters and 17.35 wt.% hydrocarbons up to C6.

Of the products derived from cold plasma decomposition of WCO, acetol is commonly used as a raw material for producing chemicals for use as lubricants and dyes [38] whereas fatty acids are used in detergents and monoglycerides are used in cosmetics and as preservatives [42]. The currently methods for producing acetol are from decomposition of glycerol and synthesis from petroleum, while fatty acids and monoglycerides are from de-esterification and pyrolysis/hydrotreatment of glycerides respectively [43]. Acetol from glycerol decomposition uses much cheaper feedstocks and is a one step process but requires specific catalysts and long reaction times [44], while synthesis from petroleum uses more costly feedstocks and requires multiple steps. In contrast, cold plasma can produce acetol from WCO selectively in a single reactor without a catalyst and with minimal further conversion to acrolein (propenal) that typically occurs during thermal production. The advantage of using cold plasma to produce fatty acids and monoglycerides is that high selectivity to a desired product can be obtained [45].

4. Conclusions

Triglycerides can be decomposed at atmospheric temperature and pressure in the presence of cold plasma without catalysts, but the yields and product selectivities are significantly improved by adding packing materials. Adding packing material such as $BaTiO_3$ increased the rate of hydrolysis reactions, resulting in a 200% increase in FA yield.

A strong synergetic effect between catalyst and cold plasma was observed. In N_2 environment Up to 40 wt.% esters (of which 31.3 wt.% was FAME) was produced from waste cooking oil at cold plasma power of 30 W and Ni/ Al_2O_3 catalyst within 7 s at ambient conditions, comparable to catalytic thermal cracking at 500 ˚C. In the presence of $BaTiO_3$ catalyst and 30 W plasma power, 51 wt.% fatty acid yields were achieved. Combining external heating to 300 ˚C and cold plasma increased conversion significantly in favour of gaseous hydrocarbons (58.8 wt.%). Zirconia and zeolites promoted the decarbonylation and decarboxylation of WCO.

H_2 environment enhanced the decomposition of glycerides, while N_2 favoured decomposition of fatty acids and esters. The overall mechanism under cold plasma was similar to conventional process via radical decomposition of triglycerides to fatty acids, glycerol and glycerides. However, due to the high energy/ low bulk temperature environment under cold plasma, an additional pathway to generate FAME and other fatty acid esters was observed though cracking the glycerol molecule backbone of the glyceride molecule, which can be promoted with cracking catalysts such as Ni/ Al_2O_3.

Declaration of Competing Interest

There are no conflicts to declare.

Data availability

Data will be made available on request.

Acknowledgements

JH would like to thank Dr Kui Zhang for his advice and guidance. This work was supported by the EPSRC, grant number OSR/0530/DT14/HARR.

References

[1] X.H. Vu, U. Armbruster, Engineering of zeolite crystals for catalytic cracking of triglycerides to renewable hydrocarbon fuels and chemicals: a review, Biomass Convers. Biorefinery (2021) 1–21.
[2] V.K. Soni, S. Dhara, R. Krishnapriya, G. Choudhary, P.R. Sharma, R.K. Sharma, Highly selective CO_3O_4/silica-alumina catalytic system for deoxygenation of triglyceride-based feedstock, Fuel 266 (2020) 117065.
[3] R. Kumar, V. Strezov, Thermochemical production of bio-oil: a review of downstream processing technologies for bio-oil upgrading, production of hydrogen and high value-added products, Renew. Sustain. Energy Rev. 135 (2021) 110152.
[4] R. El-Araby, M.A. Ibrahim, E. Abdelkader, E.H. Ismail, Co/Zn) Al_2O_4 Nano catalyst for waste cooking oil catalytic cracking, Sci. Rep. 12 (2022) 6667.
[5] H. Wang, G. LI, K. Rogers, H. Lin, Y. Zheng, S. Ng, Hydrotreating of waste cooking oil over supported CoMoS catalyst – catalyst deactivation mechanism study, Mole. Catal. 443 (2017) 228–240.
[6] E. Kozliak, M. Sulkes, I. Alhroub, A. Kubátová, A. Andrianova, W. Seames, Influence of early stages of triglyceride pyrolysis on the formation of PAHs as coke precursors, Phys. Chem. Chem. Phys. 21 (2019) 20189–20203.
[7] X. Liu, Y. Wu, J. Zhang, Y. Zhang, X. LI, H. Xia, F. Wang, Catalytic pyrolysis of nonedible oils for the production of renewable aromatics using metal-modified HZSM-5 catalysts, ACS Omega 7 (2022) 18953–18968.
[8] J. Xu, F. Long, J. Jiang, F. LI, Q. Zhai, F. Wang, P. Liu, J. Li, Integrated catalytic conversion of waste triglycerides to liquid hydrocarbons for aviation biofuels, J. Clean. Prod. 222 (2019) 784–792.
[9] S. Bezergianni, A. Dimitriadis, A. Kalogianni, P.A. Pilavachi, Hydrotreating of waste cooking oil for biodiesel production. Part I: effect of temperature on product yields and heteroatom removal, Bioresour. Technol. 101 (2010) 6651–6656.
[10] J. Harris, A.N. Phan, K. Zhang, Cold plasma catalysis as a novel approach for valorisation of untreated waste glycerol, Green Chem. 20 (2018) 2578–2587.
[11] K. Zhang, G. Zhang, X. Liu, A.N. Phan, K. Luo, A study on CO_2 decomposition to CO and O2 by the combination of catalysis and dielectric-barrier discharges at low temperatures and ambient pressure, Ind. Eng. Chem. Res. 56 (2017) 3204–3216.
[12] A. Fridman, Plasma chemistry, Cambridge University Press, 2008.
[13] W.S. Abdul-Majeed, G.S. Aal-Thani, J.N Al-Sabahi, Application of flying jet plasma for production of biodiesel fuel from wasted vegetable oil, Plasma Chem. Plasma Process. 36 (2016) 1517–1531.
[14] G. Abdulkareem-Alsultan, N. Asikin-Mijan, G. Mustafa-Alsultan, H.V. Lee, K. Wilson, Y.H. Taufiq-Yap, Efficient deoxygenation of waste cooking oil over Co_3O_4–La_2O_3-doped activated carbon for the production of diesel-like fuel, RSC Adv. 10 (2020) 4996–5009.
[15] I. Istadi, T. Riyanto, L. Buchori, D.D. Anggoro, R.A. Saputra, T.G. Muhamad, Effect of temperature on plasma-assisted catalytic cracking of palm oil into biofuels, Int. J. Renew. Energy Dev. 9 (2020) 107–112.
[16] M.A. Bashir, S. Wu, J. Zhu, A. Krosuri, M.U. Khan, R.J. Ndeddy Aka, Recent development of advanced processing technologies for biodiesel production: a critical review, Fuel Process. Technol. 227 (2022) 107120.
[17] M.G. Kulkarni, A.K. Dalai, Waste cooking oil - An economical source for biodiesel: a review, Ind. Eng. Chem. Res. 45 (2006) 2901–2913.
[18] D.L. Baulch, M.J. Pilling, C.J. Cobos, R.A. Cox, C. Esser, P. Frank, T. Just, J.A. Kerr, J. Troe, R.W. Walker, J. Warnatz, Evaluated kinetic data for combustion modelling, J. Phys. Chem. Ref. Data 21 (1992) 411–734.
[19] E. San Fabián, L. Pastor-Abia, Theoretical investigation of excited states of molecules. An application on the nitrogen molecule, Theor. Chem. Acc. 118 (2007) 637–642.
[20] A.M. Harling, J.C. Whitehead, K. Zhang, NOx formation in the plasma treatment of halomethanes, J. Phys. Chem. A 109 (2005) 11255–11260.
[21] Y.S. Choi, Y. Elkasabi, P.C. Tarves, C.A. Mullen, A.A. Boateng, Catalytic cracking of fast and tail gas reactive pyrolysis bio-oils over HZSM-5, Fuel Process. Technol. 161 (2017) 132–138.
[22] Y. Fan, Y. Cai, X. Li, H. Yin, L. Chen, S. Liu, Regeneration of the HZSM-5 zeolite deactivated in the upgrading of bio-oil via non-thermal plasma injection (NTPI) technology, J. Anal. Appl. Pyrolys. 111 (2015) 209–215.
[23] W. Charusiri, W. Yongchareon, T. Vitidsant, Conversion of used vegetable oils to liquid fuels and chemicals over HZSM-5, sulfated zirconia and hybrid catalysts, Korean J. Chem. Eng. 23 (2006) 349–355.
[24] H. Zhang, F. Zhu, X. Li, K. Cen, C. Du, X. Tu, Enhanced hydrogen production by methanol decomposition using a novel rotating gliding arc discharge plasma, RSC Adv. 6 (2016) 12770–12781.
[25] C.H. Bartholomew, R.J. Farrauto, Chemistry of nickel-alumina catalysts, J. Catal. 45 (1976) 41–53.
[26] C.H. Bartholomew, M. Rahmati, M.A. Reynolds, Optimizing preparations of Co Fischer-Tropsch catalysts for stability against sintering, Appl. Catal. A 602 (2020) 117609.
[27] R.T. Shrestha, R.B. Tyata, D.P Subedi, Estimation of electron temperature in atmospheric pressure dielectric barrier discharge using line intensity ratio method, Kathmandu Univ. J. Sci. Eng. Technol. 8 (2012) 37–42.
[28] X. Zhu, Z. Xu, Q. Liu, Q. Wang, The effect of the activation of carboxyl group and hydrogen migration on reaction pathway during the pyrolysis of triglycerides, Int. J. Green Energy 17 (2020) 676–686.
[29] C. Li, T. Liu, Q. Wang, Z. Huang, C. Xiang, Decomposition analysis of camellia oil under electric fields: an experimental and molecular simulation study, Mod. Phys. Lett. B 34 (2020) 2050431.
[30] M.M. Sein, Z. Bin Nasir, U. Telgheder, T.C. Schmidt, Studies on a non-thermal pulsed corona plasma between two parallel-plate electrodes in water, J. Phys. D Appl. Phys. (2012) 45.

[31] R.J. Buszek, A. Sinha, J.S. Francisco, The isomerization of methoxy radical: intramolecular hydrogen atom transfer mediated through acid catalysis, J. Am. Chem. Soc. 133 (2011) 2013–2015.
[32] O. Koeta, N. Blin-Simiand, W. Faider, S. Pasquiers, A. Bary, F. Jorand, Decomposition of acetaldehyde in atmospheric pressure filamentary nitrogen plasma, Plasma Chem. Plasma Process. 32 (2012) 991–1023.
[33] F. Ouni, A. Khacef, J.M. Cormier, Syngas production from propane using atmospheric non-thermal plasma, Plasma Chem. Plasma Process. 29 (2009) 119–130.
[34] V.V. Bokade, G.D. Yadav, Transesterification of edible and nonedible vegetable oils with alcohols over heteropolyacids supported on acid-treated clay, Ind. Eng. Chem. Res. 48 (2009) 9408–9415.
[35] E.B. Hemings, C. Cavallotti, A. Cuoci, T. Faravelli, E. Ranzi, A detailed kinetic study of pyrolysis and oxidation of glycerol (propane-1,2,3-triol), Combust. Sci. Technol. 184 (2012) 1164–1178.
[36] G. Knothe, M.O. Bagby, T.W. Ryan, T.J. Callahan, Degradation of unsaturated triglycerides injected into a pressurized reactor, J. Am. Oil Chem. Soc. 68 (1991) 259–267.
[37] C.M. Piqueras, D.E. Damiani, S.B. Bottini, Effect of phase behavior in the hydrogenation of triglycerides under supercritical and near-critical propane, J. Supercrit. Fluids 50 (2009) 128–137.
[38] X. Li, Z. Zhou, D. Xie, G. Chen, Preparation of acetol from crude glycerol of biomass-based via catalytic reactive distillation, Taiyangneng Xuebao/Acta Energ. Sol. Sinica 30 (2009) 1159–1162.
[39] M.H. Cho, T.Y. Mun, Y.K. Choi, J.S. Kim, Two-stage air gasification of mixed plastic waste: olivine as the bed material and effects of various additives and a nickel-plated distributor on the tar removal, Energy 70 (2014) 128–134.
[40] M. Milina, S. Mitchell, J. Perez-Ramirez, Prospectives for bio-oil upgrading via esterification over zeolite catalysts, Catal. Today 235 (2014) 176–183.
[41] J. Weitkamp, Zeolites and catalysis, Solid State Ionics 131 (2000) 175–188.
[42] N.R. Rarokar, S. Menghani, D. Kerzare, P.B. Khedekar, Progress in synthesis of monoglycerides for use in food and pharmaceuticals, J. Exp. Food Chem. 3 (2017) 1–6.
[43] P. Manara, A. Zabaniotou, Co-valorization of crude glycerol waste streams with conventional and/or renewable fuels for power generation and industrial symbiosis perspectives, Waste Biomass Valorization 7 (2016) 135–150.
[44] S. Basu, A.K. Sen, A review on catalytic dehydration of glycerol to acetol, ChemBioEng Rev. 8 (2021) 633–653.
[45] L. Di, Z. Li, B. Lee, D.W. Park, An alternative atmospheric-pressure cold plasma method for synthesizing Pd/P25 catalysts with the assistance of ethanol, Int. J. Hydrog. Energy 42 (2017) 11372–11378.